Nonlinear Dynamics and Neuroscience

Article DOI: 10.18500/0869-6632-003215

Three realizations of one neuron: variation of behavior regimes for a electronic generator of neuron-like activity in a hardware experiment

L. V. Takaishvili[1,2]✉, *A. A. Grishchenko*[2], *M. V. Sysoeva*[2], *V. I. Ponomarenko*[1,3], *I. V. Sysoev*[2,1]

[1]Saratov State University, Russia
[2]Peter the Great St. Petersburg Polytechnic University, Russia
[3]Saratov Branch of Kotelnikov Institute of Radioengineering and Electronics of RAS, Russia
E-mail: ✉nar7187@yandex.ru, vili_von@mail.ru, bobrichek@mail.ru, ponomarenkovi@gmail.com, ivssci@gmail.com

Received 4.02.2026, accepted 6.03.2026, available online 10.03.2026, published 31.03.2026

Abstract. The *purpose* of this work is to compare dynamical modes in the ensemble of hardware electronic generators of neuron-like activity with dynamical modes in SPICE simulator and mathematical model in order to detect whether the difference in oscillation amplitude, form and bifurcation value of control parameter between the hardware generators and simulation is a result of model imperfection, or this difference can be explained by features of the used electronic elements. *Models and methods.* Mathematical models, SPICE simulations and three hardware copies of the tunable generator are considered. The dependence of the excitation threshold and the oscillation amplitude on the control parameter is determined for different nonlinearities due to the number of diodes in the feedback loop. The mutual information function is used to compare the waveform. *Results.* It is shown that the existing differences can be fully explained by standard variations in the parameters of semiconductor components and other circuit elements used for the construction of electronic neurons. In this case, the simulation model can be considered as one of the generators, the parameters of which could be precisely controlled, and its components had zero tolerances. *Conclusion.* Modern simulation models are able to give a fairly good description of a full-scale experiment, it is impossible to distinguish the time series of the simulator from the experimental ones; at the same time, the experimental implementations themselves may differ due to random variations in the properties of the components.

Keywords: neuron, tunable pulse generatos, SPICE simulation, time series, diode, van der Pol oscillator.

Acknowledgements. This study was supported by Russian Science Foundation, grant No. 25-12-00176, https://rscf.ru/project/25-12-00176/.

For citation: Takaishvili LV, Grishchenko AA, Sysoeva MV, Ponomarenko VI, Sysoev IV. Three realizations of one neuron: variation of behavior regimes for a electronic generator of neuron-like activity in a hardware experiment. Izvestiya VUZ. Applied Nonlinear Dynamics. 2026;34(2):299–313. DOI: 10.18500/0869-6632-003215

Introduction

The creation of artificial neurons could potentially have a number of important applications. These are the creation of new types of artificial neural networks for the construction of human-like artificial intelligence [1], neuroprosthetics and neurorehabilitation [2], verification of models of the nervous system of living organisms, etc. In addition to applied tasks, hardware models of neural networks and systems are

also necessary for conducting fundamental research aimed at understanding the work of the brain. Since the appearance of the first hardware realization, many circuits of electronic neurons have been developed. Some of them were improvements to the original scheme proposed by Mahowald and Douglas [3], for example [4, 5]. Later, schemes based on various mathematical models were implemented, such as the FitzHugh–Nagumo model, the Morris–Lecar model, as well as simplified versions of the Hodgkin–Huxley model using electronic components. Since the nonlinear functions in the FitzHugh–Nagumo model are the simplest, in most cases hardware realizations somehow approximate it directly [6–8] or take the basic principles of organization from it [9, 10] due to the simplicity of its realization.

Hardware realizations constructed by the method of circuit modeling of equations, as in works [7, 8], theoretically should be quite stable in terms of parameters (this issue is actually poorly studied), since the approximation of nonlinear functions in them relies on direct analogues of mathematical functions: addition and multiplication using hardware methods. With modern components, this should work relatively accurately at low frequencies ranging from hundreds of hertz to tens of kilohertz, on which such neurons operate. This does not apply to models based on the approximation of nonlinear functions by the current–voltage characteristics of semiconductor elements, such as diodes, as is done in works [9, 10], since when designing neurons in this case, very approximate theoretical characteristics are implied. Although the structural stability of the constructed models often makes it possible to obtain modes close to the original ones, and even work with relatively large ensembles of such hardware neurons [11], it is still not clear how much the basic oscillation modes depend on a specific realization.

When developing electronic generators of neuron-like activity, simulators of electronic circuits [12] are often used, for example, `Multisim`, `LtSPICE` or `ngSPICE`. The quality of such simulations may depend on many factors, including the degree of elaboration of the models of individual components in them. Of course, even the most realistic models approximate the components uniquely, while in an actual experiment, the properties of diodes and transistors will differ, even if they are taken from the same batch. Construction hardware neural networks involves both scaling up the production of individual electronic neurons and, as a necessary step, construction models of such networks in simulators to control the results, eliminate installation errors, and simplify the study of dynamics. In this regard, an important question arises: are the differences observed between the signals of electronic neurons in simulators and (if available) mathematical models the result of the imperfections of such models, or are they the result of variations in specific instances of semiconductor elements used in the actual experiment?. In fact, we can ask: is the model in the simulator, in terms of the generated signals, one of the instances of electronic neurons (simply because all parameters were accurately controlled for this instance), or is it fundamentally different from the actual realizations because significant systematic inaccuracies were introduced during its construction? The purpose of this study is to answer this question for a promising model developed in [9].

1. Methods

1.1. Circuit modeling. The simulation was performed in the open-source circuit simulator `ngSPICE` [12]. Since `ngSPICE` itself is a solver of systems of equations and a component library, but not a development environment, the environment `QUQS-S` [13] that is currently being actively developed, including by domestic developers, was used as a visual assistant. The FitzHugh–Nagumo neuron circuit published in [10] was used as a basis. This circuit was then reduced in [9], resulting in a more than twofold reduction in the number of circuit components while adding a signal shape control element through a variable number of diodes and increasing the pulse duty cycle, making the generation modes more neuron-like. Fig. 1 shows the neuron circuit developed in [9].

Next, three hardware realizations of this circuit were created. The models and component values of all three realizations were identical. The components, such as diodes, capacitors, and inductor coils, were taken from the same batch. Fig. 2 shows the hardware realizations of the three generators.

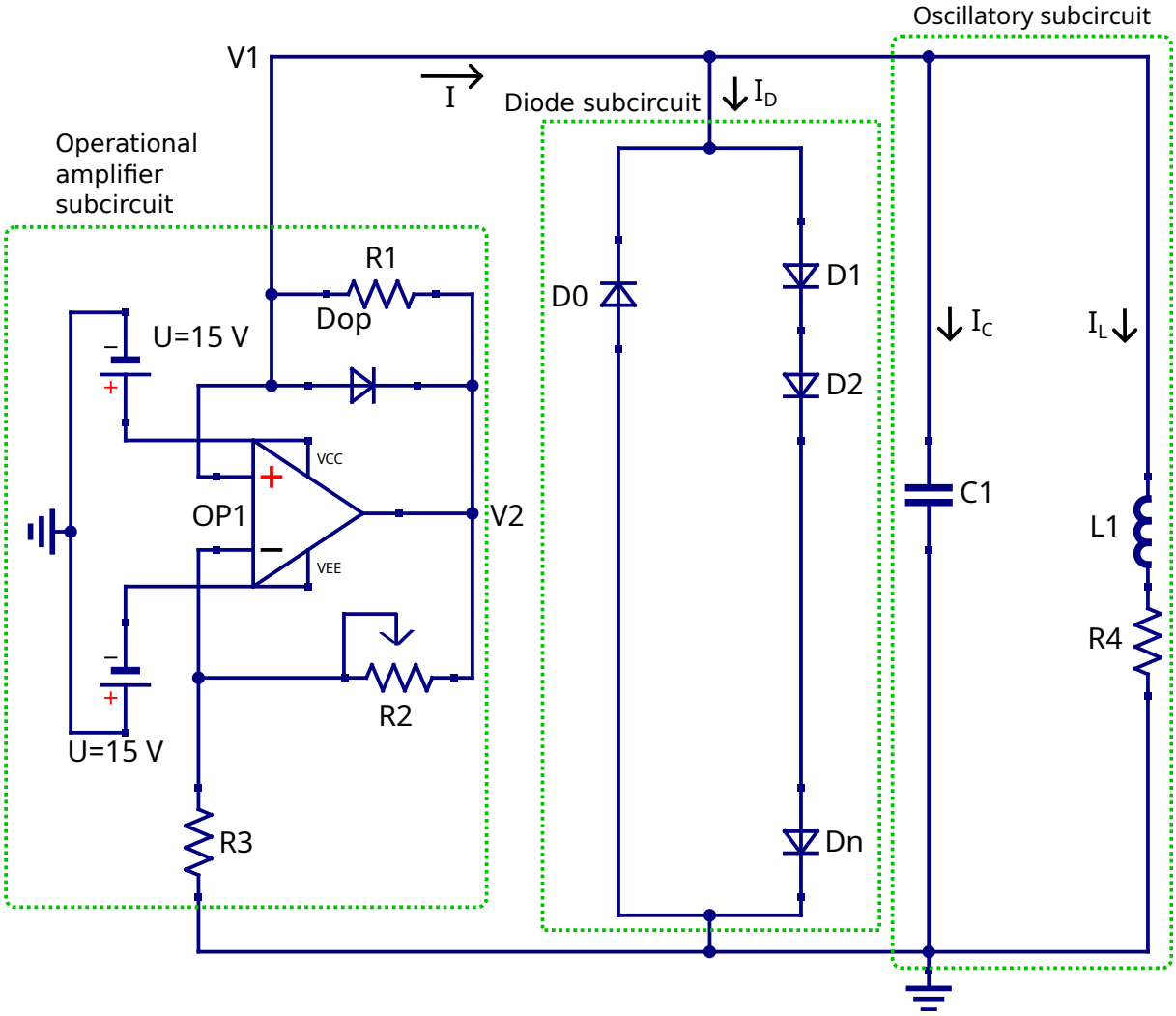

Fig. 1. Circuit diagram of the simple tunable generator of neuron-like activity. Operational amplifier subcircuit consist of operational amplifier $OP1$ of type LM358, resistors $R_1 = 1$ $k\Omega$ and $R_3 = 1$ $k\Omega$, potentiometer R_2, diode D_{op} of type 1N4148. Diode subcircuit consists of $n + 1$ diodes of type 1N4148. Oscillatory subcircuit consists of capacitor $C_1 = 300$ nF, inductor coil $L_1 = 1$ mH, resistor $R_1 = 2$ Ω (color online)

1.2. Mathematical model of an electronic neuron. The mathematical model of the developed generator is actually a generalized van der Pol generator, which can be written as follows:

$$\frac{d^2V_1}{dt^2} + \frac{dV_1}{dt}\left(\frac{R_4}{L_1} + \frac{\rho + \rho_D}{C_1} + \frac{1}{C_1}V_1\left(\frac{d\rho}{dV_1} + \frac{d\rho_D}{dV_1}\right)\right) + \\ + \frac{1}{L_1C_1}V_1\left(1 + (\rho + \rho_D)R_4\right) = 0, \tag{1}$$

where ρ is the conductivity of the operational amplifier subcircuit, and ρ_D is the conductivity of the diode subcircuit. At small amplitudes (in linear modes), all diodes are closed, so the conductivity $\rho_D \to 0$, and in the operational amplifier subcircuit, the current flows only through the resistor R_1, but not through the diode D_{op}, so subcircuit conductivity can be expressed as $\rho = -\frac{R_2}{R_1R_3}$ (for more details, see the derivation based on Kirchhoff equations in [9]), which is simply a constant responsible for amplifying oscillations, it is an external energy source or negative friction. In this case, the dependence of ρ on the applied voltage disappears, and therefore, $\frac{d\rho}{dV_1} = 0$. Thus, in linear modes, including near the bifurcation value of the

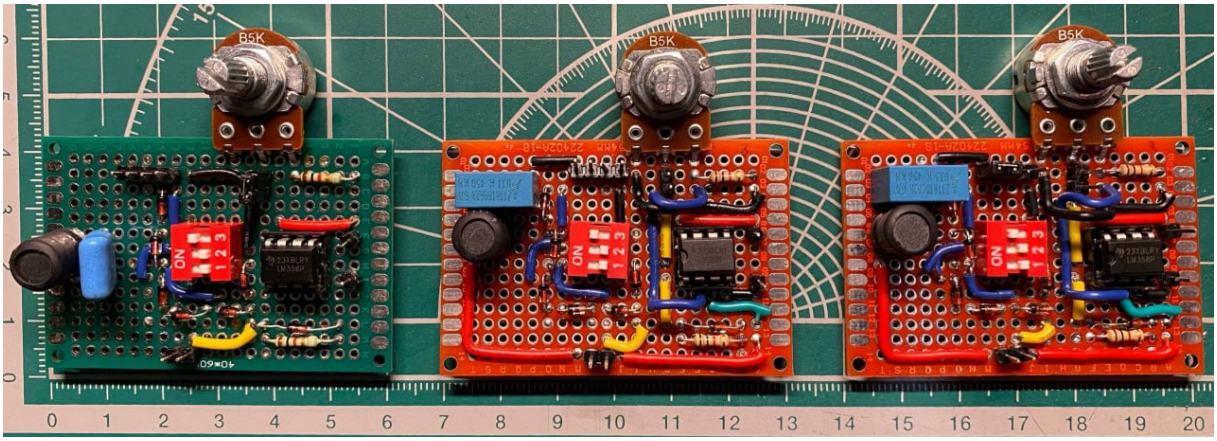

Fig. 2. The photo of three different items — hardware realizations of the simple tunable generator of neuron-like activity (color online)

parameter R_2 responsible for the supercritical Andronov–Hopf bifurcation, the model equations can be approximated by the equation of a linear dissipative oscillator:

$$\frac{d^2V_1}{dt^2} + \frac{dV_1}{dt}\left(\frac{R_4}{L_1} - \frac{R_2}{R_1R_3C_1}\right) + \frac{1}{L_1C_1}V_1\left(1 - \frac{R_2}{R_1R_3}R_4\right) = 0. \tag{2}$$

It is obvious that the excitation condition for such an oscillator is the equality of zero to the coefficient before the first derivative, that is:

$$\frac{R_4}{L_1} = \frac{R_2}{R_1R_3C_1}. \tag{3}$$

This relationship corresponds to the loss of stability of a focus and the birth of a cycle. As we can see, it is affected by the values of most of the resistors, the capacitor, and the inductor coil, including the potentiometer R_2 and the inductor coil resistance R_4, and it directly follows from (3) that R_2 is proportional to R_4, which is relatively small (2 Ω).

1.3. Mutual information function. The mutual information function was used to evaluate the similarity of the waveform. The mutual information function MI is a universal measure of the similarity of two experimental samples X (consisting of the values $\{x_i\}_{i=1}^N$) and Y (consisting of the values $\{y_i\}_{i=1}^N$). It is important here that each x_i has its own y_i associated, that is, these are precisely pairs of values that can be indicated by points on the (X, Y) plane. Traditionally, the mutual information function is defined in terms of joint $H_{X,Y}$ and individual H_X and H_Y entropies as follows:

$$MI_{X,Y} = H_X + H_Y - H_{X,Y}. \tag{4}$$

It is often used for signal analysis; in this case, we talk about non-directional connectivity or synchrony, including because the measure is sensitive to the frequency difference of the signals under consideration, just like the correlation function, but it reveals both linear and nonlinear dependencies.

The direct method of calculating MI using formula (4) requires estimating all three entropies from experimental data: H_X, H_Y and $H_{X,Y}$, for example, by dividing the entire measurement area into bins and counting the hits in each bin. but this approach can lead to big errors and requires huge amounts of data. Therefore, in practice, it is not the mutual information function itself that is calculated, but its estimate, for example, the so-called Kozachenko–Leonenko entropy [14]. This is exactly the approach described in [15], and is used in this article. To speed up calculations, the sorting algorithm described in [16] is used.

To calculate the Kozachenko-Leonenko estimate, neighbors are searched for each i-th point ($i = 1, \ldots, N$) on the (X, Y) plane, and the distance between the i-th and j-th points is defined as the maximum of the coordinates' distances, using formula (5):

$$d_{i,j} = \max(|x_i - x_j|, |y_i - y_j|). \tag{5}$$

Next, the K-th neighbor in terms of proximity is found, and the distance to it is denoted by $\varepsilon/2$. Then, the number of neighbors is calculated separately for X — n_X and for Y — n_Y. In this work, $K = 4$.

With this method of introducing the distance, it is asymptotically unbiased, that is, for $N \to \infty$ having a mathematical expectation equal to the true value of MI, the estimate of the mutual information function can be calculated using the following formula:

$$MI_{xy} = \psi(N) + \psi(K) - \langle \psi(n_x(i) + 1) + \psi(n_y(i) + 1) \rangle_i , \tag{6}$$

where $\psi(n)$ is the digamma function.

2. Results

2.1. Visual signal analysis. Signals from all three hardware realizations were recorded for different numbers of diodes ($n = 1, 3, 5$) and at different resistor resistance R_2 (changed from 500 Ω to 1600 Ω in 50 Ω increments). Similarly, time realizations for the mathematical model and the simulation model from the ngspice simulator were recorded.

To begin with, let us consider the dependence of the amplitude of the signal voltage on the resistance of the control resistor R_2 (Fig. 3) for one, three and five diodes connected in the forward direction in the diode subcircuit. Since it was originally assumed that the oscillations should be highly nonlinear, the range between the minimum and maximum values of the signal was taken as the «amplitude». The main differences between the curves are in the resistance at which oscillations occur. Moreover, the moment of oscillation for each specific realization does not depend on the number of diodes in the diode subcircuit. In mathematical and simulation models, oscillations occur at $R_2 \approx 600$ Ω. The three physical realizations showed different results relative to each other and to virtual models. The first neuron has oscillations at $R_2 \approx 900$ Ω, while the second and third have oscillations at $R_2 \approx 750$ Ω. These differences can be easily explained within the framework of the bifurcation ratio (3) by the fact that the actual resistance of the inductor coil turned out to be higher than the nominal in all realizations, and a slight deviation, by tenths of an ohm, leads to a significant, by hundreds of ohm, a shift in R_2 since , all other things being equal, R_4 is 500 times less than R_2. This is an obvious weak point of the circuit, which can be eliminated by, for example, increasing the nominal value of R_4 and simultaneously reducing the nominal value of R_3 or R_1 by the same amount. At the same time, this disadvantage does not significantly affect the nonlinear

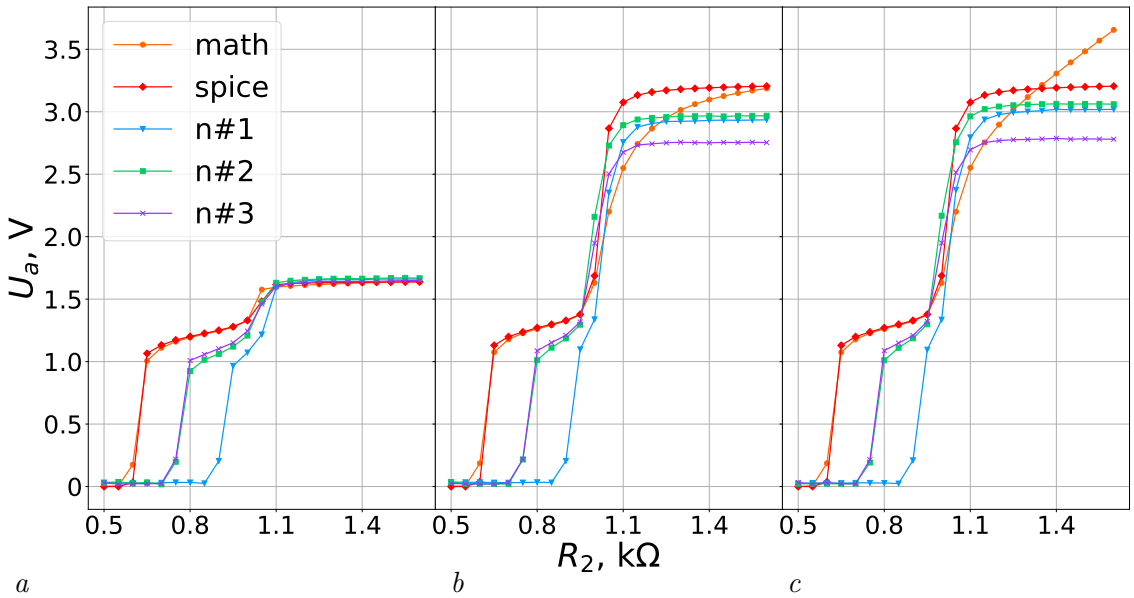

Fig. 3. Dependance of voltage amplitude of resistance in controlling resistor R_2. a — $n = 1$; b — $n = 3$; c — $n = 5$. Orange line corresponds to the mathematical model, red line — to the ngspice simulation, blue line — to the neuron #1, green line — to the neuron #2, purple line — neuron #3 (color online)

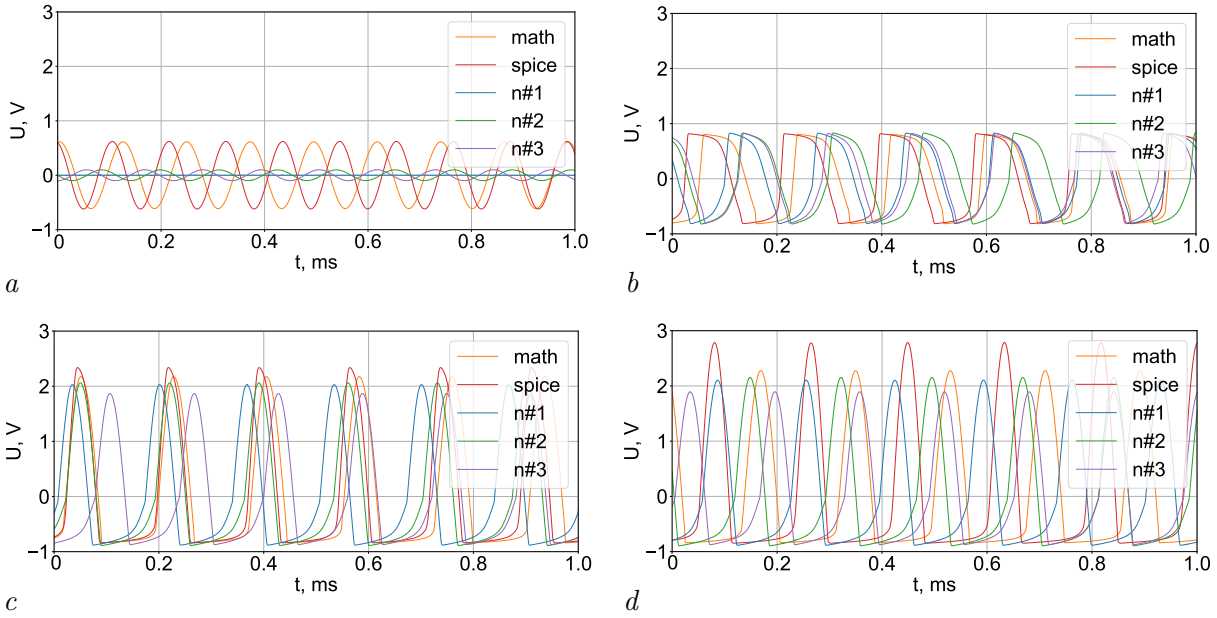

Fig. 4. Time series of the circuit output voltage V1 at: a — $R_2 = 750\ \Omega$ ($n = 1, 3, 5$); b — $R_2 = 1300\ \Omega$ ($n = 1$); c — $R_2 = 1300\ \Omega$ ($n = 3$); d — $R_2 = 1300\ \Omega$ ($n = 5$). Orange line corresponds to the mathematical model, red line — to the ngspice simulation, blue line — to the neuron #1, green line — to the neuron #2, purple line — neuron #3 (color online)

target modes for the generator under consideration, that is, it is not significant.

Next, all the graphs show a sharp increase in the oscillation amplitude to $U_a \approx 1$ V. Then, the oscillation amplitude increases slowly (for the mathematical and simulation models), slightly faster (for neurons № 2 and № 3), or almost instantly (for neuron № 1) to a value that is approximately the same for different realizations, but varies for different numbers of diodes in the diode subcircuit. When the number of diodes is $n = 1$, the amplitude increases to $U_a \approx 1.6$ V, and when $n = 3$ and $n = 5$, the amplitude increases to $U_a \approx 2.9 \pm 0.2$ V.

Next, let us look at the waveform, to do this, let us pay attention to the signals themselves at several characteristic values of R_2: 750 Ω (the moment of the first sharp increase in amplitude for neurons № 2 and № 3) and 1300 Ω (the moment of reaching the second «plateau» of the oscillation amplitude of all three hardware neurons). The time realizations for small R_2 (up to about 900 Ω) look the same for all the diodes considered in the work ($n = 1, 3, 5$). Fig. 4, a it can be seen that when the value $R_2 = 750\ \Omega$ is mathematical (meaning full model (1), although in this mode its oscillations are visually indistinguishable from the oscillations of reduced model (2)) and simulation models already demonstrate sinusoidal oscillations of high amplitude, neurons № 2 and № 3 demonstrate sinusoidal oscillations, but still of small amplitude, and neuron № 1 is still in the subthreshold mode. At values of $R_2 > 900\ \Omega$, the number of diodes connected to the diode subcircuit already affects the final waveform. Fig. 4 b, c, d shows that at $R_2 = 1300\ \Omega$, the amplitude increases with increasing number of diodes in the circuit. The waveform also depends on the number of diodes in the diode subcircuit.

2.2. Quantitative signal analysis. In this work, our main task is to evaluate the degree of similarity or difference of signals received from three hardware realizations of neurons, as well as from mathematical and simulation models with the same circuit parameters (the same number of diodes, the same ratings of all resistors and potentiometers). First, let us estimate the spectral composition of the signals.

The amplitude spectrum were constructed at $R_2 = 750\ \Omega$ and $R_2 = 1300\ \Omega$ for one, three, and five diodes in a diode subcircuit. At $R_2 = 750\ \Omega$, the spectra predictably look the same (Fig. 5, a) for all the diodes considered in the work ($n = 1, 3, 5$). These are linear oscillations, and there are no higher harmonics of the main oscillation frequency on the spectra. Fig. 5 b, c, d shows the amplitude spectra of

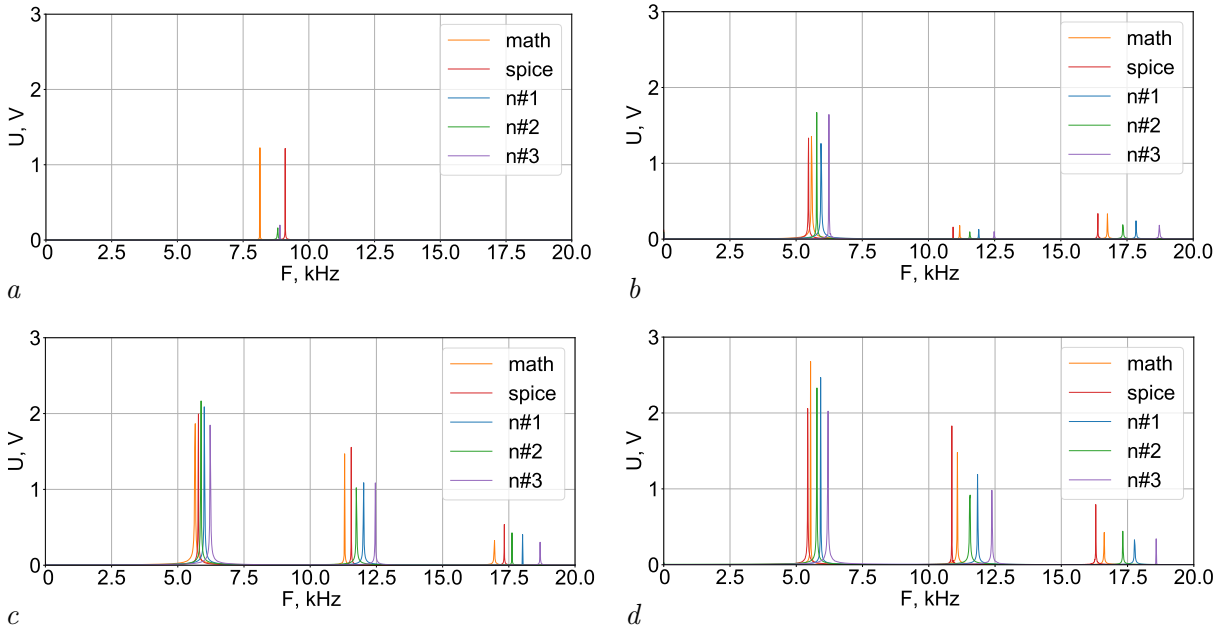

Fig. 5. Amplitude spectrum for signal of the circuit output voltage V1 at: a — $R_2 = 750$ Ω ($n = 1, 3, 5$); b — $R_2 = 1300$ Ω ($n = 1$); c — $R_2 = 1300$ Ω ($n = 3$); d — $R_2 = 1300$ Ω ($n = 5$). Orange line corresponds to the mathematical model, red line — to the ngspice simulation, blue line — to the neuron #1, green line — to the neuron #2, purple line — neuron #3 (color online)

the output voltage signal at the nominal value of the controlling resistor $R_2 = 1300$ Ω for one (Fig. 5, b), three (Fig. 5, c) and five (Fig. 5, d) «direct» in the diode subcircuit. Firstly, the spectra show that the received signals are highly nonlinear — the second and third harmonics of the signal are well expressed, and the larger the n, the more energy is contained in the higher harmonics. Secondly, it can be seen that at $n \geqslant 3$ the spectral structure no longer changes. Thirdly, it can be seen that the spectral structure for all three hardware realizations of the neuron, as well as mathematical and simulation models, is very similar, although the main oscillation frequencies are slightly different (Table 1). It was calculated by how many percentages the obtained frequencies differ from each other using the symmetric percentage difference formula: $d_{xy} = \frac{2|f_x - f_y|}{(f_x + f_y)} \cdot 100\%$, where x is the first system, f_x is the main oscillation frequency of the first system, y is the second system, f_y is the main oscillation frequency of the second system.

Table 1. The main oscillation frequency for signal of the circuit output voltage V1

F, kHz	$R_2 = 750$ Ω					$R_2 = 1300$ Ω				
	math	spice	n#1	n#2	n#3	math	spice	n#1	n#2	n#3
$n = 1$	8.10	9.10	0	8.80	8.90	5.60	5.45	5.90	5.80	6.20
$n = 3$	8.10	9.10	0	8.80	8.90	5.70	5.80	6.00	5.90	6.20
$n = 5$	8.10	9.10	0	8.80	8.90	5.50	5.45	5.90	5.80	6.20

According to the Table 2 it is clearly seen that the frequencies of all five considered signals differ by no more than 13% for any values of R_2 and n used. At the same time, the main signal frequencies of the hardware realizations differ from each other by a maximum of 7%. The maximum difference is observed between the frequency of the third neuron and the frequencies of the mathematical and simulation models.

Since our task is to evaluate the similarity of the waveform, rather than its main frequency, for each time realization, the time was adjusted for the oscillation period (the time series was purposefully divided into $T = 1/F$). As a result, the characteristic period of all signals began to occupy 1 conventional unit. Unfortunately, after this operation, the direct application of the mutual information function became impossible, since now the sampling step has become unique in each signal and there are no simultaneous

Table 2. Symmetrical percentage difference of the signal main frequencies. Lower indexes: m — mathematical model, s — ngspice simulation, 1 — neuron #1, 2 — neuron #2, 3 — neuron #3

R_2, Ω	Diodes	d_{ms}	d_{m1}	d_{m2}	d_{m3}	d_{s1}	d_{s2}	d_{s3}	d_{12}	d_{13}	d_{23}
750	1, 3, 5	12 %	—	8 %	9 %	—	3 %	2 %	—	—	1 %
1300	$n = 1$	3 %	5 %	4 %	10 %	8 %	6 %	13 %	2 %	5 %	7 %
	$n = 3$	2 %	5 %	3 %	8 %	3 %	2 %	7 %	2 %	3 %	5 %
	$n = 5$	1 %	7 %	5 %	12 %	8 %	6 %	13 %	2 %	5 %	7 %

values. Therefore, cubic spline interpolation was performed next, and all five realizations were resampled with the same new sampling frequency. For this purpose, the functions `splev` and `splrep` from the module `interpolate` of the package `scipy` were used [17]. It was these re-selected series that were used to compare the degree of similarity based on an assessment of the mutual information function. It should be noted that this method also made it possible to get rid of the dependence on the quantization step and the ratio of the dynamic range of the ADC to the oscillation range.

Table 3. Evaluation of the mutual information function MI. Lower indexes: m — mathematical model, s — ngspice simulation, 1 — neuron #1, 2 — neuron #2, 3 — neuron #3

	$R_2 = 750$ Ω			$R_2 = 1300$ Ω		
	$n = 1$	$n = 3$	$n = 5$	$n = 1$	$n = 3$	$n = 5$
MI_{ms}	1.241	1.181	1.195	1.248	1.284	1.354
MI_{m1}	0.835	0.813	0.810	1.468	1.493	1.339
MI_{m2}	1.194	1.330	1.181	1.301	1.200	1.235
MI_{m3}	1.598	1.224	1.385	1.275	1.234	1.269
MI_{s1}	0.837	0.821	0.818	1.256	1.877	1.663
MI_{s2}	1.221	1.291	1.277	1.380	1.266	1.366
MI_{s3}	1.480	1.272	1.276	1.599	1.313	1.252
MI_{12}	0.461	0.280	0.165	1.489	1.252	1.275
MI_{13}	0.501	0.284	0.235	1.377	1.482	1.537
MI_{23}	1.269	1.257	1.284	1.408	1.275	1.267

Table 3 clearly shows that when the signals are clearly not similar (neuron №1 does not oscillate at $R_2 = 750$ Ω), the mutual information function is less than one, in all other cases $1 < MI < 2$. If we compare three samples with each other at $R_2 = 1300$ Ω: hardware realizations with each other (MI_{12}, MI_{13}, MI_{23}), a mathematical model with hardware realizations (MI_{m1}, MI_{m2}, MI_{m3}), a simulation model with hardware realizations (MI_{s1}, MI_{s2}, MI_{s3}), then it is clearly seen that their distributions overlap. That is, hardware realizations differ from each other as much as they differ from mathematical and simulation models.

Conclusion

Simulators of electronic circuits (also known as SPICE) have been used for many years to simulate various nonlinear devices, including chaos generators [18–20]. A significant number of results related to hidden attractors in electronic systems were also obtained using simulators [21]. At the same time, it is still not clear to what extent such simulators accurately reproduce the modes in the real scheme. In particular, the question remains open as to how much the inaccuracy of setting component values in a full-scale experiment affects the difference between simulation and experimental signals.

The work done shows that the models of semiconductor elements embedded in modern simulators are generally quantitatively adequate for describing modes, including highly nonlinear (pulse) ones, characteristic of electronic neurons. We can assume that the model in the simulator is an ideal representative of its class, for which it was possible to accurately set the values of individual elements. Obviously, this is not possible in the case of real devices, and moreover, we face the problem of using non-identical identical elements in the same installation, rather than just non-identical elements in different instances of the generator under consideration. It is important that the simulator shows not only qualitatively and quantitatively (in terms of the shape of the oscillations) similar time series, but also gives a very similar curve to the experimental dependence of the oscillation range on the control parameter, including for an asymmetric diode subcircuit. At the same time, the existing quantitative differences in the amplitude of the oscillations and the bifurcation value are easily explained precisely by the inaccuracy of setting the parameters of the generators.

At the same time, the mathematical model constructed in [9], is obviously somewhat simplified compared to the simulator, demonstrating signals similar in shape, inaccurately reproduces the curve of the oscillation range depending on the magnitude of the gain (control parameter), showing growth where saturation is present in the simulator and in the full-scale experiment. For electronic neurons constructed using semiconductor elements to directly describe their nonlinear functions (for example, due to their current–voltage characteristics), the problem of having an adequate mathematical model has always occurred.

References

1. Levi T, Nanami T, Tange A, Aihara K, Kohno T. Development and applications of biomimetic neuronal networks toward brainmorphic artificial intelligence. IEEE Transactions on Circuits and Systems II: Express Briefs. 2018;65(5):577–581. DOI: 10.1109/TCSII.2018.2824827.
2. Park HL, Lee Y, Kim N, Seo DG, Go GT, Lee TW. Flexible neuromorphic electronics for computing, soft robotics, and neuroprosthetics. Adv. Mater. 2020;32(15):1903558. DOI: 10.1002/adma.201903558.
3. Mahowald M, Douglas R. A silicon neuron. Nature. 1991;354:515–518. DOI: 10.1038/354515a0.
4. Rasche C, Douglas R. An improved silicon neuron. Analog Integr. Circ. Sig. Process. 2000;23:227–236. DOI: 10.1023/A:1008357931826.
5. van Schaik A. Building blocks for electronic spiking neural networks. Neural Netw. 2001; 14(6–7):617–628. DOI: 10.1016/S0893-6080(01)00067-3.
6. Li F, Liu Q, Guo H, Zhao Y, Tang J, Ma J. Simulating the electric activity of FitzHugh–Nagumo neuron by using Josephson junction model. Nonlinear Dyn. 2012;69:2169–2179. DOI: 10.1007/s11071-012-0417-z.
7. Kulminskiy DD, Ponomarenko VI, Prokhorov MD, Hramov AE. Synchronization in ensembles of delay-coupled nonidentical neuronlike oscillators. Nonlinear Dyn. 2019;98:735–748. DOI: 10.1007/s11071-019-05224-x.
8. Egorov NM, Sysoev IV, Ponomarenko VI, Sysoeva MV. Complex regimes in electronic neuron-like oscillators with sigmoid coupling. Chaos, Solitons and Fractals. 2022;160:112171. DOI: 10.1016/j.chaos.2022.112171.
9. Takaishvili LV, Ponomarenko VI, Sysoev IV. Simple tunable generator of neuron-like activity. Chaos, Solitons and Fractals. 2025;196:116316. DOI: 10.1016/j.chaos.2025.116316.
10. Binczak S, Kazantsev VB, Nekorkin VI, Bilbault JM. Experimental study of bifurcations in modified FitzHugh-Nagumo cell. Electronics Letters. 2003;39(13):961–962. DOI: 10.1049/el:20030657.
11. Binczak S, Jacquir S, Bilbault JM, Kazantsev VB, Nekorkin VI. Experimental study of electrical FitzHugh–Nagumo neurons with modified excitability. Neural Netw. 2006;19(5): 684–693. DOI: 10.1016/j.neunet.2005.07.011.
12. Madec M, Lallement C, Haiech J. Modeling and simulation of biological systems using SPICE language. PLoS ONE. 2017;12(8):e0182385. DOI: 10.1371/journal.pone.0182385.
13. Brinson ME, Kuznetsov VV. Extended behavioural device modelling and circuit simulation with

Qucs-S. International Journal of Electronics. 2018;105(3):412–425. DOI: 10.1080/00207217.2017.1357764.
14. Kozachenko LF, Leonenko NN. Sample estimate of the entropy of a random vector. Problems of Information Transmission. 1987;23(2):95–101.
15. Kraskov A, Stögbauer H, Grassberger P. Estimating mutual information. Phys. Rev. E. 2004;69(6):66–138. DOI: 10.1103/PhysRevE.69.066138.
16. Sysoev IV. Comparison of numerical realisation of algorithm of mutual information calculation based on nearest neighbours. Izvestiya VUZ. Applied Nonlinear Dynamics. 2016;24(4): 86–95. DOI: 10.18500/0869-6632-2016-24-4-86-95.
17. Virtanen P, Gommers R, Oliphant TE, Haberland M, Reddy T, Cournapeau D, Burovski E, Peterson P, Weckesser W, Bright J, van der Walt SJ, Brett M, Wilson J, Millman KJ, Mayorov N, Nelson ARJ, Jones E, Kern R, Larson E, Carey CJ, Polat İ, Feng Y, Moore EW, VanderPlas J. SciPy 1.0: fundamental algorithms for scientific computing in Python. Nat. Methods. 2020;17(3):261–272. DOI: 10.1038/s41592-019-0686-2.
18. Kuznetsov SP. Electronic circuits manifesting hyperbolic chaos and simulation of their dynamics using software package multisim. Izvestiya VUZ. Applied Nonlinear Dynamics. 2011;19(5): 98–115. DOI: 10.18500/0869-6632-2011-19-5-98-115.
19. Kuznetsov SP. Plykin type attractor in electronic device simulated in MULTISIM. Chaos. 2011;21(4):043105. DOI: 10.1063/1.3646903.
20. Kuznetsov SP. Simple electronic chaos generators and their circuit simulation. Izvestiya VUZ. Applied Nonlinear Dynamics. 2018;26(3):35–61. DOI: 10.18500/0869-6632-2018-26-3-35-61.
21. Kuznetsov NV, Leonov GA, Yuldashev MV, Yuldashev RV. Nonlinear analysis of classical phase-locked loops in signal's phase space. IFAC Proceedings Volumes. 2014;47(3):8253–8258. DOI: 10.3182/20140824-6-ZA-1003.02772.